

Gibbs-ensemble Monte Carlo simulation of H₂-He mixturesArmin Bergermann, Martin French , Manuel Schöttler, and Ronald Redmer 
Institut für Physik, Universität Rostock, 18051 Rostock, Germany (Received 29 September 2020; accepted 24 November 2020; published 12 January 2021)

We explore the performance of the Gibbs-ensemble Monte Carlo simulation technique by calculating the miscibility gap of H₂-He mixtures with analytical exponential-six potentials. We calculate several demixing curves for pressures up to 500 kbar and for temperatures up to 1800 K and predict a H₂-He miscibility diagram for the solar He abundance for temperatures up to 1500 K and determine the demixing region. Our results are in good agreement with *ab initio* simulations in the nondissociated region of the phase diagram. However, the particle number necessary to converge the Gibbs-ensemble Monte Carlo method is yet too large to offer a feasible combination with *ab initio* electronic structure calculation techniques, which would be necessary at conditions where dissociation or ionization occurs.

DOI: [10.1103/PhysRevE.103.013307](https://doi.org/10.1103/PhysRevE.103.013307)

I. INTRODUCTION

Hydrogen and helium are not only the first and simplest elements in the Periodic Table, but also the most abundant materials in gas giant planets like Jupiter and Saturn [1,2]. Recent *ab initio* calculations predict that H₂-He mixtures phase separate at 1–2 Mbar, i.e., at conditions in the upper envelope of Jupiter and Saturn [3–6]. This demixing process leads to the formation of He-rich droplets sinking toward the planetary core. The *ab initio* predictions explain not only the reduced He fraction x_{He} in the atmosphere of Jupiter and Saturn compared to the protosolar value of $Y = 0.28$ [1], but also Saturn's excess luminosity [7–9]. The sinking droplets convert gravitational energy into heat, which contributes to the luminosity and delays the cooling of the planet. If this demixing process is neglected, most evolution models of Saturn yield a planetary age substantially lower than that of the solar system [3]. The consideration of demixing processes under extreme pressure and temperature conditions is therefore crucial for the development of improved models of gas giant planets [10,11].

Loubeyre *et al.* [12] measured demixing in the H₂-He system at pressures of $p < 60$ kbar at room temperature by using diamond anvil cells. So far, no experiments indicating demixing at conditions relevant for jovian planets have been published. Schouten *et al.* [13] performed Gibbs-ensemble Monte Carlo simulations to calculate the miscibility gap of H₂-He mixtures. They predicted two demixing curves at $T = 1000$ and 1500 K and found separation at pressures of $p = 230$ and 385 kbar at the lower and higher temperatures, respectively. Additionally, they predicted a demixing line for H₂-He at temperatures of $T \leq 2500$ K and at pressures of $p \lesssim 750$ kbar.

Recently, research has been carried out by using *ab initio* methods to calculate demixing by evaluating differences in the Gibbs free energy ΔG [3–6,14,15]. Lorenzen *et al.* [4] calculated the H₂-He phase diagram for arbitrary He fractions considering the ideal entropy of mixing. This simple

approximation has already led to good results at $p \gtrsim 1$ Mbar but is questionable at pressures of $p \lesssim 1$ Mbar. Morales *et al.* [5,6] conducted similar simulations, but also considered the nonideal entropy to determine the demixing phase diagram for solar He abundance, and obtained a demixing line lower than that of Lorenzen *et al.* [4]. Both of these studies employed *ab initio* simulation methods based on density-functional theory (DFT). The central approximation in DFT is the choice of the exchange-correlation (XC) functional, which determines how accurately the quantum mechanical electronic interactions are captured. While both Lorenzen *et al.* [4] and Morales *et al.* [5,6] used the semilocal Perdew-Burke-Ernzerhof [16] functional, a more recent paper by Schöttler and Redmer [3] used a nonlocal van der Waals XC functional [17] and also considering the nonideal entropy found an even lower demixing line in the pressure-temperature plane than Morales *et al.* [5,6]. These most recent calculations predict H₂-He phase separation to occur in Saturn but not in Jupiter. The intricate correlation between the H₂-He phase diagram, in particular the location of the demixing region, and the evolution of Jupiter and Saturn has been studied in detail recently (see [11]).

Nevertheless, performing *ab initio* calculations is computationally expensive, in particular at the lower pressure and temperature regime. Therefore, we use the Gibbs-ensemble Monte Carlo simulation method of Panagiotopoulos *et al.* [18–20] in this study in order to determine the region where H₂-He mixtures phase separate. Unlike studies based on DFT, our results are limited to mixtures of H₂ molecules and He atoms. First, we calculate two demixing curves at temperatures of $T = 1000$ and 1500 K in order to compare our results with those of Schouten *et al.* [13]. Second, we extend the demixing diagram of Schöttler and Redmer [3] to the lower-temperature and -pressure regime. We calculate demixing curves at pressures of $100 \text{ kbar} \leq p \leq 500 \text{ kbar}$ and at temperatures of $T \lesssim 1800$ K. Third, we predict a demixing phase diagram for solar He abundance. In Secs. II and III we briefly explain the simulation technique used in this work.

TABLE I. Parameters for the exponential-six potential (5) regarding the H₂-H₂, H₂-He, and He-He interactions.

Interaction	ϵ (kJ/mol)	r^M (Å)	α	Ref.
H ₂ -H ₂	0.302646	3.43	11.1	[25]
H ₂ -He	0.143840	3.28	12.49	[26]
He-He	0.089763	2.9673	13.1	[27]

In Sec. IV we present our results and compare with previous calculations and experiments. Section V gives a summary.

II. SIMULATION METHOD

In this section we briefly explain the Gibbs-ensemble Monte Carlo (GEMC) method. A more detailed description is given in Refs. [13,18–20]. This technique is based on two separate simulation boxes which contain $N_{I,II}^A$ particles of species A and $N_{I,II}^B$ particles of species B. The indices I and II denote boxes I and II, respectively. The total number of particles $N^A = N_I^A + N_{II}^A$ and $N^B = N_I^B + N_{II}^B$ is conserved. The boxes have different volumes V_I and V_{II} but the same temperature T and the same external pressure p .

The GEMC process evolves the spatial configurations of particles in both simulation boxes in different ways and attempts to simulate a thermal equilibrium state at constant pressure and constant temperature. First, an attempt is made to displace particles within each of both boxes. Second, an attempt is made to resize the volume in order to keep the average pressure constant. Third, particle transfers and particle swaps between the boxes are attempted.

Particle displacement. Every particle is randomly displaced within a maximum allowed distance. The well-known acceptance probability [18] is given by

$$\mathbb{P}_{PD} = \min[1, \exp(-\beta\Delta E)], \quad (1)$$

where $\Delta E = E_{\text{new}} - E_{\text{old}}$ defines the change in energy and $\beta = 1/k_B T$.

Volume change. In order to keep the average pressure constant, we attempt to resize the volumes of both boxes independently within $0 < \Delta V < \Delta V_{\text{max}}$. The acceptance probability was derived in [21,22] and is given by

$$\mathbb{P}_{VC} = \min\left\{1, \exp\left[-\left(\beta\Delta E - N \ln \frac{V + \Delta V}{V} + \beta p \Delta V\right)\right]\right\}, \quad (2)$$

where ΔV denotes the change in volume.

Particle transfer. A random particle of species A or B contained in either of the boxes I or II is transferred to a random position in the other box. The respective acceptance probability is similar to that for particle insertions in the grand canonical ensemble and given by [18–20]

$$\mathbb{P}_{PT} = \min\left\{1, \exp\left[-\beta\left(\Delta E_I + \Delta E_{II} + \frac{1}{\beta} \ln \frac{V_{II}(N_I^A + 1)}{V_I N_{II}^A}\right)\right]\right\}, \quad (3)$$

where $\Delta E_I = E_{I,\text{new}} - E_{I,\text{old}}$ and $\Delta E_{II} = E_{II,\text{new}} - E_{II,\text{old}}$. The acceptance probability of transfer steps is quite low at high densities; thus, many transfers will be rejected. The

excluded-volume map sampling method [23] was used to avoid the computational expensive calculation of the change in energy ΔE .

Particle swap. Essentially, the so-called particle swap is a transfer of two particles of different species between the two boxes [13,24]. First, a random particle of species A or B contained in either of the boxes I or II is chosen. Second, one randomly selects a particle of the other species in the other box. The selected particles may swap their species, whereas their positions remain the same. The acceptance probability of such a swap is given by

$$\mathbb{P}_{PS} = \min\left\{1, \exp\left[-\beta\left(\Delta E_I + \Delta E_{II} + \frac{1}{\beta} \ln \frac{V_{II}(N_I^A + 1)}{V_I N_{II}^A} + \frac{1}{\beta} \ln \frac{V_I(N_{II}^B + 1)}{V_{II} N_I^B}\right)\right]\right\}. \quad (4)$$

III. SIMULATION DETAILS

We used exponential-six potentials

$$\Phi_{ij}(r) = \frac{\epsilon_{ij}}{\alpha_{ij} - 6} \left\{ 6 \exp\left[\alpha_{ij} \left(1 - \frac{r}{r_{ij}^M}\right)\right] - \alpha_{ij} \left(\frac{r_{ij}^M}{r}\right)^6 \right\} \quad (5)$$

to model the interactions in the H₂-He system. The parameters α_{ij} , r_{ij}^M , and ϵ_{ij} are given in Table I. The H₂-H₂ potential is calibrated to shock compression data for pressures up to 750 kbar and temperatures up to 7000 K [25]. The He-He potential is likewise calibrated to shock compression data for pressures up to 120 kbar and temperatures up to 300 K. To extend its applicability to even higher pressures, Young *et al.* [26] performed linear muffin-tin orbital electron-band-theory calculations. Due to the absence of internal degrees of freedom in the He atom, we regard the potential to be valid also at temperatures of several 1000 K. The H₂-He potential is calibrated to diamond anvil cell data for pressures up to 75 kbar and pressures up to 360 K by van den Bergh and Schouten [27].

Initially, we placed 8192 He atoms and 8192 H₂ molecules on simple cubic lattices in each of the boxes. The simulations consisted of 10 000 steps for internal equilibration inside each box, during which we attempted to displace all particles and tried to resize the volumes of both boxes to reach the desired pressure. This internal equilibration process was followed by 40 000 global steps. During a global step, we attempted to displace all particles and resize the volumes. Additionally, 20 000 particle transfers and 2000 particle swaps were tried. After the global equilibrium was reached (usually after 10 000 steps for equilibration), the molar fractions of the species in each box were calculated by averaging until the simulation end. The

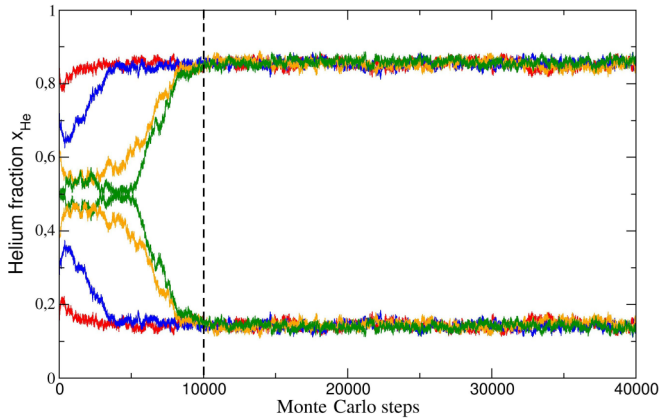


FIG. 1. The GEMC simulation for a H_2 -He mixture at $T = 1400$ K and $p = 400$ kbar. The different colors depict four different initial conditions regarding the concentrations of x_{He} and x_{H_2} . The concentration averaging starts after 10 000 Monte Carlo steps (black dashed line).

large number of 40 000 steps was chosen to diminish errors due to large fluctuations or an insufficiently demixed system. We started the first simulation at high-pressure conditions far away from the lowest pressure at which demixing occurs. After each run, we started a new simulation run at lower pressure conditions until we found H_2 -He to be completely miscible.

In extensive convergence tests, we found that particle numbers $\gtrsim 16384$ are necessary in order to obtain converged results with deviations of less than 1.5%. Because the computational power in 1991 was much more limited than ours today, Schouten *et al.* [13] had to perform their simulations with only 256 He atoms and 256 H_2 molecules and were unable to perform extensive convergence tests with more particles. With such small particle numbers, we observed that the boxes swap “identities” during the simulations several times, i.e., from box I rich in x_{He} and poor in x_{H_2} to box I rich in x_{H_2} and poor in x_{He} , and vice versa for box II. This takes place especially close to the lowest pressure at which demixing occurs.

For each pressure-temperature condition, we ran four simulations with different initial concentrations in box I and box II of x_{He} and x_{H_2} . The situation is depicted in Fig. 1 with four different colors. This method made it easy to detect metastable states or huge fluctuations.

In Fig. 1 a simulation run at a temperature of $T = 1400$ K and a pressure of $p = 400$ kbar is shown. The system is demixed after 10 000 Monte Carlo steps (black dashed line). The average molar fractions are $x_{\text{He}} \approx 0.78$ (box I) and $x_{\text{He}} \approx 0.14$ (box II).

IV. RESULTS AND DISCUSSION

First, we simulated two demixing curves at $T = 1000$ and 1500 K, depicted in Figs. 2 and 3, respectively. The demixing pressures are given as a function of the He fraction x_{He} . Compared to Schouten *et al.* [13], we used a much larger number of particles, which resulted in a much smaller statistical uncertainty. A comparison of the lowest pressure at which demixing

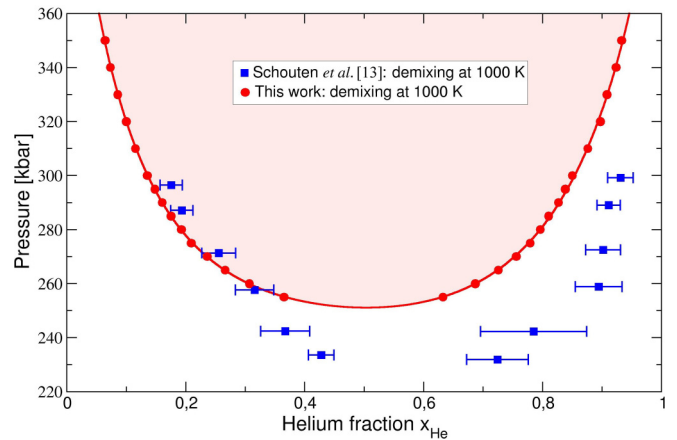


FIG. 2. Demixing curve for H_2 -He at $T = 1000$ K as derived from GEMC simulations. The red circles are the results of this work, while the blue squares are those of Schouten *et al.* [13]. The red line is a smoothing spline acting as a guide to the eye. Demixing occurs under conditions within the red shaded area.

occurs is shown in Table II. Our calculations indicate highly symmetric demixing curves, likely due to the purely radial form of all interaction potentials used. The asymmetry in the curves predicted by Schouten *et al.* is probably an artifact generated by insufficiently converged simulation data. Moreover, our calculations predict a higher lowest pressure at which demixing occurs than Schouten *et al.* [13]. By performing test calculations with 150 000 Monte Carlo steps and the same low particle number ($N = 512$) as Schouten *et al.* [13], we found huge fluctuations regarding the concentrations of x_{He} and x_{H_2} . Within these fluctuations we could reproduce the results of Schouten *et al.* [13].

Second, we simulated five demixing curves at pressures of $100 \text{ kbar} \leq p \leq 500 \text{ kbar}$. The results are depicted in Fig. 4. Because it was not feasible, Schöttler and Redmer [3] did not perform any *ab initio* simulations at pressures below 500 kbar. The colored diamonds at $x_{\text{He}} = 1$ are the He melting

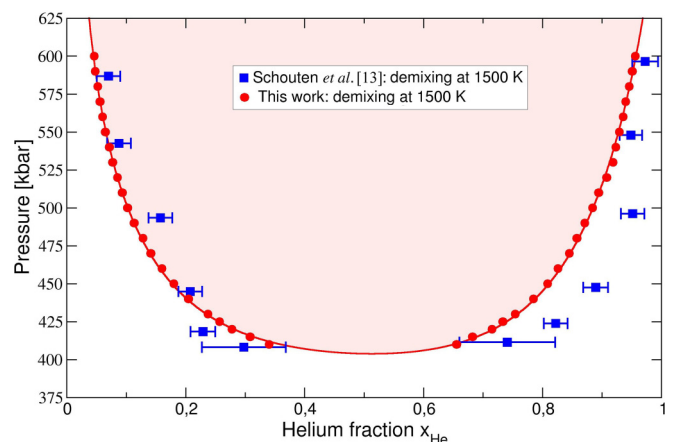


FIG. 3. Demixing curve for H_2 -He at $T = 1500$ K as derived from GEMC simulations. The red circles are the results of this work, while the blue squares are those of Schouten *et al.* [13]. The red line is a smoothing spline acting as a guide to the eye. Demixing occurs under conditions within the red shaded area.

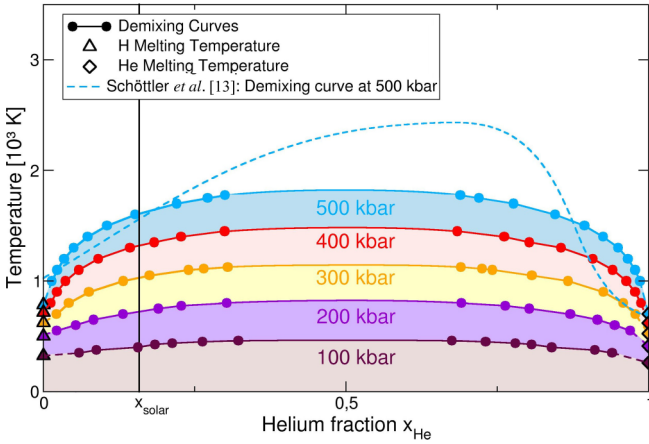


FIG. 4. Miscibility diagram of H₂-He mixtures as derived from GEMC simulations (colored circles). The lines are smoothing splines acting as guides to the eye. Demixing occurs under conditions within the shaded areas. The dashed line is the result of Schöttler and Redmer [3] using DFT-MD simulations. The vertical black line indicates the solar He concentration as relevant for Fig. 6. Colored triangles and diamonds show the melting temperature of pure H₂ [29] and He [28], respectively.

temperatures as calculated by Preising and Redmer [28]. The colored triangles at $x_{\text{He}} = 0$ are the H₂ melting temperatures [29]. Our demixing curves are highly symmetric, while the result at $p = 500$ kbar of Schöttler and Redmer [3] shows an asymmetric behavior with a kink towards higher He fractions. The *ab initio* data show an abrupt increase of the demixing temperature at low hydrogen fractions at $n_{\text{H}}^{1/3} a_B \approx 0.25$, which represents the concentration required to transform hydrogen to a metal according to the Mott criterion [4]. In *ab initio* simulations, metallization of hydrogen is the driving force of the demixing process at high pressures, which leads to asymmetric demixing curves. At moderate pressures, where hydrogen is yet mostly molecular, the asymmetry in the *ab initio* demixing data can be explained with (i) the molecular structure of hydrogen vs the atomic structure of helium and (ii) the difference in interaction strength between these species, i.e., helium is mostly repulsive while interactions with H₂ are a little more attractive (see Table II). Inserting a low concentration of hydrogen into helium thus has little effect on ΔG , but the presence of low He concentration in H₂ disturbs the interactions between H₂ molecules more strongly, depending on the pressure [30]. Part of the reason is perturbations of the intramolecular vibrations, which are detectable in the contribution of nuclear quantum effects to ΔG , as explained in Chap. 3.2. of Ref. [30]. The purely radial interaction potentials used in this work cannot capture such effects, so the *ab*

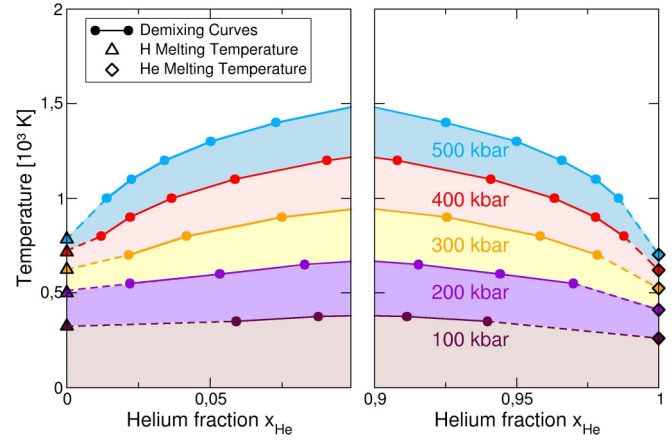


FIG. 5. Miscibility diagram of H₂-He mixtures for very high and very low He concentrations. The colored circles connected by solid lines are the results of the GEMC simulations. The dashed lines connect the GEMC results with the H₂ and He melting temperatures [28] shown by colored triangles and colored diamonds, respectively.

initio demixing curve at 500 kbar is likely the more reliable one.

Figure 5 compares the H₂ melting temperatures by Morales *et al.* [29] and the He melting temperatures by Preising and Redmer [28] to our demixing curves. The demixing temperature is given as a function of the He fraction. It is not meaningful to use the GEMC method at temperatures below the melting point. Particle insertions and removals of single particles fail for crystalline phases because they involve the creation of interstitial or vacancy defects [31]. Thus, we were not able to simulate a fully demixed system of pure solid He and pure H₂. The compression behavior at dense H₂-He mixtures in the solid phase was studied recently by x-ray diffraction [32]. Nevertheless, the dashed lines that connect our results to the H₂ [29] and He [28] melting points can likewise be regarded as reasonable extrapolation of our results to $x_{\text{He}} = 0$ and 1. Hence our GEMC simulations are in alignment with a fully demixed system for temperatures below the melting temperature of H₂ and He, which Schöttler and Redmer [3] also predicted in their *ab initio* simulations.

Because the exponential-six potential shows an unphysical behavior at small intermolecular distances it was not possible to simulate even higher pressures and temperatures. This limitation was already discussed in more detail by Schouten *et al.* [13]. Nevertheless, our work agrees with earlier *ab initio* results [3–6,14,15] reasonably well at conditions where no dissociation or ionization occurs. Finally, we calculated the demixing diagram for the solar He abundance of $Y = 0.28$ at temperatures of $T \lesssim 1500$ K. The results are shown in Fig. 6.

TABLE II. Lowest pressure at which demixing occurs at temperatures of $T = 1000$ and 1500 K. The results of this work are compared with the results of Schouten *et al.* [13].

Temperature T (K)	Schouten <i>et al.</i>	This work
1000	$p = 230$ kbar at $x_{\text{H}_2} = 0.4$	$p = 250$ kbar at $x_{\text{H}_2} = 0.5$
1500	$p = 385$ kbar at $x_{\text{H}_2} = 0.45$	$p = 400$ kbar at $x_{\text{H}_2} = 0.5$

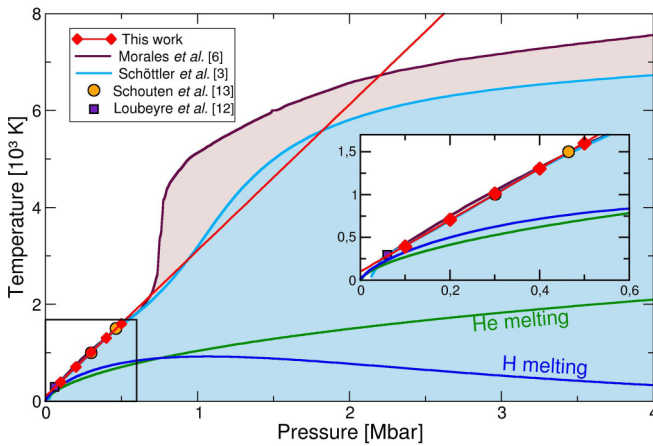


FIG. 6. Miscibility diagram at the solar He abundance of $Y = 0.28$. Red diamonds depict results of this work obtained with the GEMC method and the red line is a linear fit towards higher temperatures. Colored areas show results of *ab initio* simulations performed by Schöttler and Redmer (lower blue area) [3] and Morales *et al.* (upper violet area) [6]. The magenta square depicts the experimental result of Loubeyre *et al.* [12] and the orange circle the result of Schouten *et al.* [13]. At low temperatures the melting lines for H_2 [29] and He [28] are shown for the sake of orientation. The inset shows the results at the p - T domain considered here.

The red diamonds are the results of this work, which are in very good agreement with the experimental data of Loubeyre *et al.* [12] and *ab initio* results of Refs. [3,6]. Interestingly, the deviation between the results of Schouten *et al.* [13] and

ours is relatively small in the pressure-temperature diagram, despite the poor convergence of their simulations.

V. CONCLUSION

In summary, we have used GEMC simulations to examine the H_2 -He phase diagram at pressures of $100 \text{ kbar} \leq p \leq 500 \text{ kbar}$ and temperatures of $T \lesssim 1800 \text{ K}$. In doing so, we extended the hydrogen-helium miscibility diagram of Schöttler *et al.* [3] to lower pressures. Our GEMC simulations indicate a fully demixed system below the He melting temperature and reproduce earlier results obtained from *ab initio* methods [3–6] with a significantly different approach. Although the pressures and temperatures considered in this work do not overlap with Jupiter’s or Saturn’s interior conditions, our findings facilitate efforts to understand physical processes that lead to demixing of hydrogen and helium in astrophysical objects. Our results are in agreement with experiments of Loubeyre *et al.* [12] and should stimulate further demixing experiments toward higher pressures and temperatures. Technically, we found the GEMC method not yet suitable to be combined with *ab initio* electronic structure calculations in order to determine miscibility diagrams because of the very high particle number needed to achieve convergence.

ACKNOWLEDGMENTS

We thank Mandy Bethkenhagen and Hanns-Peter Liermann for helpful discussions. This work was supported by the Deutsche Forschungsgemeinschaft via the Research Unit FOR 2440 and by Deutsches Elektron-Synchrotron (DESY) Hamburg via the Centre for Molecular Water Science.

- [1] U. von Zahn, D. M. Hunten, and G. Lehmacher, *J. Geophys. Res.* **103**, 22815 (1998).
- [2] B. J. Conrath, D. Gautier, R. A. Hanel, and J. S. Hornstein, *Astrophys. J.* **282**, 807 (1984).
- [3] M. Schöttler and R. Redmer, *Phys. Rev. Lett.* **120**, 115703 (2018).
- [4] W. Lorenzen, B. Holst, and R. Redmer, *Phys. Rev. Lett.* **102**, 115701 (2009).
- [5] M. Morales, E. Schwegler, D. Ceperley, C. Pierleoni, S. Hamel, and K. Caspersen, *Proc. Natl. Acad. Sci. USA* **106**, 1324 (2009).
- [6] M. A. Morales, S. Hamel, K. Caspersen, and E. Schwegler, *Phys. Rev. B* **87**, 174105 (2013).
- [7] D. J. Stevenson and E. E. Salpeter, *Astrophys. J. Suppl.* **35**, 221 (1977).
- [8] J. J. Fortney, *Science* **305**, 1414 (2004).
- [9] R. Püstow, N. Nettelmann, W. Lorenzen, and R. Redmer, *Icarus* **267**, 323 (2016).
- [10] D. J. Stevenson, *Phys. Rev. B* **12**, 3999 (1975).
- [11] C. R. Mankovich and J. J. Fortney, *Astrophys. J.* **889**, 51 (2020).
- [12] P. Loubeyre, R. Letoullec, and J. Pinceaux, *J. Phys.: Condens. Matter* **3**, 3183 (1991).
- [13] J. A. Schouten, A. de Kuijper, and J. P. J. Michels, *Phys. Rev. B* **44**, 6630 (1991).
- [14] O. Pfaffenzeller, D. Hohl, and P. Ballone, *Phys. Rev. Lett.* **74**, 2599 (1995).
- [15] W. Lorenzen, B. Holst, and R. Redmer, *Phys. Rev. B* **84**, 235109 (2011).
- [16] J. P. Perdew, K. Burke, and M. Ernzerhof, *Phys. Rev. Lett.* **77**, 3865 (1996).
- [17] M. Dion, H. Rydberg, E. Schröder, D. C. Langreth, and B. I. Lundqvist, *Phys. Rev. Lett.* **92**, 246401 (2004).
- [18] A. Z. Panagiotopoulos, *Mol. Phys.* **61**, 813 (1987).
- [19] A. Panagiotopoulos, N. Quirke, M. Stapleton, and D. Tildesley, *Mol. Phys.* **63**, 527 (1988).
- [20] A. Z. Panagiotopoulos, *Mol. Simul.* **9**, 1 (1992).
- [21] D. Frenkel and B. Smit, *Understanding Molecular Simulation: From Algorithms to Applications*, 2nd ed. (Academic, San Diego, 2002).
- [22] M. Allen and D. Tildesley, *Computer Simulation of Liquids* (Oxford University Press, Oxford, 1987).
- [23] G. L. Deitrick, L. E. Scriven, and H. T. Davis, *J. Chem. Phys.* **90**, 2370 (1989).
- [24] J. de Pablo and J. Prausnitz, *Fluid Phase Equilibr.* **53**, 177 (1989).
- [25] M. Ross, F. H. Ree, and D. A. Young, *J. Chem. Phys.* **79**, 1487 (1983).

- [26] D. A. Young, A. K. McMahan, and M. Ross, *Phys. Rev. B* **24**, 5119 (1981).
- [27] L. C. van den Bergh and J. A. Schouten, *J. Chem. Phys.* **89**, 2336 (1988).
- [28] M. Preising and R. Redmer, *Phys. Rev. B* **100**, 184107 (2019).
- [29] M. A. Morales, C. Pierleoni, E. Schwegler, and D. M. Ceperley, *Proc. Natl. Acad. Sci. USA* **107**, 12799 (2010).
- [30] M. Schöttler and R. Redmer, *J. Plasma Phys.* **85**, 945850201 (2019).
- [31] B. Chen, J. I. Siepmann, and M. L. Klein, *J. Phys. Chem. B* **105**, 9840 (2001).
- [32] J. Lim, M. Kim, S. Duwal, S. Kawaguchi, Y. Ohishi, H.-P. Liermann, R. Hrubiak, J. S. Tse, and C.-S. Yoo, *Phys. Rev. B* **101**, 224103 (2020).